https://doi.org/10.5194/angeo-2020-92
Preprint. Discussion started: 4 January 2021

Annales Geophysicae Discussions
Open Access
EGU

Ionospheric control of space weather

Osuke Saka
Office Geophysik, Ogoori, 838-0141, Japan

Abstract
We propose that ionospheric plasma injections to the magnetosphere (ionospheric injection) represent a new plasma process in the polar ionosphere. The ionospheric injection is first triggered by westward electric fields transmitted from the convection surge in the magnetosphere in association with dipolarization onset. Localized westward electric fields result in local accumulation of ionospheric electrons because of differing electron and ion mobility in the E-layer. This charge imbalance was quickly reduced by polarization electric fields generated in the ionosphere. Meanwhile, ion/electron populations are partially released as injections to the magnetosphere to sustain initial potential distributions in quasi-neutral equilibrium.

Resultant geomagnetic field lines are not in equipotential equilibrium during ionospheric injections but instead develop field-aligned potentials to extract ions/electrons ejected from the ionosphere. Field-aligned potential can exist in the magnetic mirror geometry of auroral field lines if the magnetospheric plasma follows quasi-neutral equilibrium. The parallel potential distribution may be global in scale varying monotonically along the field lines between the ionosphere and the equator. Amplified equatorial projection of ionospheric potentials then develop substorm dipolarization processes in a positive feedback loop. Cold plasmas from the ionosphere are distributed along the dynamical trajectories in the magnetosphere and conserve the total energy (including electrostatic potentials) and first adiabatic invariant. They distribute along a dynamical trajectory either leaving only the energetic part of ionospheric plasmas or not changing velocity space distributions from the ionospheric source.

1. Introduction

The Earth's magnetosphere is a dynamic system responding to the electromagnetic and particle energy flows from the Sun. Those energy flows deform the original magnetic field

https://doi.org/10.5194/angeo-2020-92
Preprint. Discussion started: 4 January 2021

configurations of dipole fields by enhanced plasma convections. The convections redistribute plasma populations and produce electric currents to sustain the new configurations of the Earth's magnetosphere stretching in anti-sunward directions (magnetotail). Meanwhile, stretched magnetic configurations often return to the original dipole fields discontinuously (field line dipolarization). Such discontinuous reconfigurations may be caused by disruption of cross-field electric currents [e.g., McPherron et al, 1973; Lui et al., 1996] and by relaxation of the radial inhomogeneity of the tail plasmas [Saka, 2020]. The reconfiguration produces inductive westward electric fields of the order of 1 mV/m in the dipolarization front [e.g., Runov et al., 2011]. These fields would be transmitted to the polar ionosphere and penetrate below the E layer altitudes if the horizontal scale length exceeds 1 km [Forget et al., 1991]. The fields may be detected in Balloon-flight experiments [Kelley et al., 1971], Barium release experiments [Haerendel, 1972], and incoherent scatter radar observations [Nielsen and Greenwald, 1978].

We propose in this report that the polar ionosphere responds dynamically to these incident electric fields. The dynamic response of the ionosphere shows injection of ionospheric plasmas to the magnetosphere (ionospheric injection) as well as production of field-aligned potentials and redistribution of ionospheric plasmas along these field lines. This scenario indicates a new role for the ionosphere in the M-I coupling process in the magnetosphere. The ionosphere is not merely a load in the MI-coupling system but takes the initiative in space weather.

2. Ionospheric injection and formation of field-aligned potential

The ionospheric injection scenario proposed in Saka [2019] may be briefly summarized as follows: (1) External electric fields penetrated in the polar ionosphere produce local accumulation/rarefaction of electric charges in the E-layer by the mobility difference of electrons and ions; (2) Resulting charge separation may be readily reduced by the secondary (polarization) electric fields; (3) A fraction of particle populations is released out of the ionosphere as ionospheric injections to sustain initial potential distributions in quasi-neutral equilibrium.

This ionospheric injection scenario is schematically shown in Figure 1. Ionospheric injection results in both generator and load. Localized westward electric fields ($\mathbf{E}_w$) accumulated negative charges (electrons) in lower latitudes leaving positive charges (ions) in higher latitudes because of differing electron and ion mobility in the E-layer (blue arrow, generator).

Polarization electric fields ($\mathbf{E}_p$) produced by the charge separation moved ions to lower latitudes ($\mathbf{U}_{i\perp} = b_i\mathbf{E}_p$, b_i is mobility of ions) as Pedersen currents to neutralize the

https://doi.org/10.5194/angeo-2020-92
Preprint. Discussion started: 4 January 2021

ionosphere (red arrow, load). To avoid a complete neutralization of the ionosphere, some positive charges (ions) in negative potential regions in lower latitudes and some negative charges (electrons) in positive potential regions in higher latitudes were expelled from the ionosphere. This partial neutralization process sustained original potential distributions in quasi-neutral equilibrium. In Figure 1, we do not include the Hall currents driven by the secondary polarization electric fields. The Hall current produce current vortices flowing clockwise (as viewed from above) in a positive potential region in higher latitudes and counterclockwise in negative potentials in lower latitudes [Saka, 2020].

Meanwhile, geomagnetic field lines are not in equipotential equilibrium during ionospheric injections but instead develop both downward electric fields in positive potential regions of higher latitudes to extract electrons located there and upward electric fields in negative potential regions of lower latitudes to extract ions. Parallel electric fields can exist in the magnetic mirror geometry of auroral field lines if the magnetospheric plasma follows quasi-neutral equilibrium [Alfven and Falthammar, 1963; Persson, 1963]. The resultant potential distributions in the polar ionosphere and in the magnetosphere are presented in Figure 2. Because of parallel potentials in the magnetosphere, potential difference in the ionosphere never weaken but instead amplify during their equatorial projection. Equatorial projection of southward electric fields generated earthward electric fields in the magnetosphere, which in turn introduced asymmetric expansion of field line dipolarization in dawn-dusk directions.

3. Steady-state, field-aligned transport of ionospheric species

For about 10 minutes following Pi2 onset, nighttime magnetosphere could be in a transitional state repeating local field line dipolarization [Saka et al., 2010]. In this transitional interval, steady-state motions of electrons and ions can be assumed. In guiding center approximation, one-dimensional parallel motion could be given as,

$$v_{//}\frac{\partial v_{//}}{\partial s} = G_{//} + \frac{q|e|}{m_q}E_{//} - \frac{\mu_q}{m_q}\frac{\partial B}{\partial s} \qquad (1)$$

In equation (1), $|e|$ is the charge, m_q is the mass, μ_q is the magnetic moment, $G_{//}$ is the gravitational acceleration, B is the magnetic field strength, $E_{//}$ is the parallel electric field, $v_{//}$ is the parallel velocity, and s is along field lines. Note that q=1 for ions and q=-1 for electrons. In this equation, centrifugal force is ignored. Equation (1) can be reduced to the constants of the motion (W, μ),

$$W = \frac{m_q}{2}(v_{//}^2 + v_{\perp}^2) + q|e|\Phi \qquad (2)$$

https://doi.org/10.5194/angeo-2020-92
Preprint. Discussion started: 4 January 2021

Annales Geophysicae Discussions

$$\mu = \frac{m_q}{2B} v_\perp^2 \qquad (3)$$

Here, $v_\perp$ and Φ denote perpendicular velocity and electrostatic potential along the field lines, respectively.

Gravitational term in (1) can be ignored in (2) if the electrostatic potential above the ionosphere decreased below -10 Volt.

Combination of equations (2) and (3) yields,

$$v_{//}'^2 = v_{//}^2 + (1 - B'/B) v_\perp^2 + (2q|e|/m_q)(\Phi - \Phi') \qquad (4)$$

Equation (4) gives dynamical trajectory in phase space between two points, $(v_{//}', v_\perp'; \Phi')$ and $(v_{//}, v_\perp; \Phi)$, along the same field lines [e.g., Chiu and Schulz, 1978].

If the dynamical trajectory starts from the bottom-side ionosphere, $(v_{//}', v_\perp'; \Phi')$ is at the ionospheric E layer and $(v_{//}, v_\perp; \Phi)$ is either at 1,000km, 10,000 km, 20,000 km and at geosynchronous (50,000 km) altitudes. The trajectory trace of the velocity space is shown in Figures 3 and 4.

In Figure 3, both the magnetic mirror force and parallel potential accelerated ionospheric sources. This acceleration process moved ionospheric source plasmas labelled (Σ) to the bottom-right or to the bottom-left corner in velocity space as the altitudes increased from 1,000 km to the geosynchronous altitudes. We ignored the left-hand side of the velocity space because we are only interested in the outflows from the ionosphere ($v_{//} > 0$). Figure 3 illustrates two cases: (1) Ionospheric electrons are accelerated in downward electric fields where field-aligned potential increased with increasing altitudes; (2) Ionospheric ions are accelerated in upward electric fields where the potential decreased with increasing altitudes. Assuming the Maxwell distribution function for velocity distributions of ions and electrons above 1,000 km in altitudes, in accordance with Liouville's theorem we calculate parallel and perpendicular temperatures of ionospheric species at altitudes of 1,000 km, 10,000 km, 20,000 km, and geosynchronous. The velocity distribution function of ionospheric plasmas is given by,

$$f(v_{//}, v_\perp; \Phi) = \left(\frac{m_q}{2\pi k T_q}\right)^{3/2} \exp\left(\frac{m_q}{2kT_q}(v_{//}^2 + v_\perp^2) + \frac{q|e|\Phi}{kT_q}\right) \qquad (5)$$

Here kT_q is 1 eV for ions/electrons. Electrostatic potential Φ is 0 volt at the ionosphere.

https://doi.org/10.5194/angeo-2020-92
Preprint. Discussion started: 4 January 2021

The temperature of parallel/perpendicular component in eV is given by $\frac{m_q}{2}\left\langle v_{//,\perp}^2 \right\rangle$, where

$$\left\langle v_{//,\perp}^2 \right\rangle = \frac{\int_\Sigma v_{//,\perp}^2 f(v) d^3v}{\int_\Sigma f(v) d^3v} \quad (6)$$

Integration was caried out in the velocity space (Σ) bounded by the hyperbolic curve. Note that velocity space integration was carried out only in the positive velocity area.

For both ions and electrons, parallel and perpendicular temperatures $\left(\frac{m_q}{2}\left\langle v_{//}^2 \right\rangle, \frac{m_q}{2}\left\langle v_{\perp}^2 \right\rangle\right)$ initially (0.5 eV, 1.0 eV) in the ionosphere changed to (11.3 eV, 0.70 eV) at 1,000 km where electrostatic potential was 10 V for electrons and -10 V for ions. Temperatures changed to (51.9 eV, 0.09 eV) at 10,000 km where electrostatic potential was 50 V for electrons and -50 V for ions. When electrostatic potential further increased to 200 V for electrons and decreased to -200 V for ions at 20,000 km, temperatures changed to (202.0 eV, 0.02 eV). At geosynchronous altitudes, temperatures changed to (502 eV, 0.002 eV) where potential is assumed to be 500 V for electrons and -500 V for ions. Parallel potential and mirror geometry skewed velocity space of the ionospheric source and increased parallel temperatures and decreased perpendicular ones at altitudes above the ionosphere.
The other cases where parallel potentials act as a potential barrier are shown in Figure 4. In this type, dynamical trajectories filled all velocity space in $v_{//}$, and parallel temperature (0.5 eV at the ionosphere) did not change above the ionosphere up to geosynchronous altitudes, while perpendicular temperature decreased to 0.87 eV at 20,000 km, and to 0.42 eV at geosynchronous altitudes. We conclude that accelerating potential raised parallel temperature of the escaping ionospheric species. The potential barriers did not change the parallel temperature of the ionospheric source.

4. Field-aligned current

Ions in the E layer drifted from positive potentials in higher latitudes to negative potentials in lower latitudes to discharge imbalance produced by the mobility difference. Drift velocities of these ions ($\mathbf{U}_{i\perp}$) may be given as,

$$\mathbf{u}_{i\perp} = \frac{\Omega_i}{B\nu_{in}} \mathbf{E}_p \quad (7)$$

Here, Ω_i, ν_{in}, $\mathbf{E}_p$ denote ion cyclotron frequency, ion-neutral collision frequency and secondary polarization electric fields, respectively. Substituting mean ion cyclotron and ion-

https://doi.org/10.5194/angeo-2020-92
Preprint. Discussion started: 4 January 2021

Annales Geophysicae Discussions

neutral collision frequencies in (7), we have ion drift velocities on the order of 5.9 x 10^1 m/s for electric fields of the order of 0.1 V/m. Those drifting ions carry southward Pedersen currents of the order of $1.0\mu A/m^2$ in the E-layer. These ionospheric currents might be redirected to the field-aligned currents at the northern and southern edge of the ionosphere to close 2-D current system. We therefore suggest that field-aligned currents of the order of $1.0\mu A/m^2$ may flow above the ionosphere in the ionospheric injection scenario. To test this hypothesis, we calculate the field-aligned currents along the dynamical trajectories using $\mathbf{J}_{//q} = nq|e|\langle v_{//}\rangle$, where

$$\langle v_{//}\rangle = \frac{\int_{\Sigma} v_{//} f(v) d^3v}{\int_{\Sigma} f(v) d^3v} \qquad (8)$$

The results show that electrons carry downward field-aligned currents of the order of $1.6\mu A/m^2$ at the number density $n = 10^2/m^3$. This is a fraction of the background density at the bottom-side ionosphere ($n = 10^{11}/m^3$). We conclude that upward flowing electrons may close Pedersen currents at the northern edge of the ionosphere, while upward flowing ions at the southern edge of the ionosphere could not provide enough current density to close the Pedersen currents. Therefore, electrons from the magnetosphere are necessary for closing the Pedersen currents at the southern edge of the ionosphere.

5. Summary and Discussion

In this report, we presented a new ionospheric dynamo process driven by external electric fields transmitted from the magnetosphere at the onset of field line dipolarization. The dynamo process yielded plasma injections arising out of the ionosphere (ionospheric injection). Plasma injections into the magnetosphere in turn generated field-aligned potentials on a global scale to achieve quasi-neutrality of the magnetosphere. These potentials consist of downward electric fields in the northern edge of the auroral ionosphere and upward electric fields in the southern edge of the auroral ionosphere. In the downward electric field region, ionospheric electrons carried field-aligned currents downward, while in the upward electric field region, magnetospheric electrons carry field-aligned currents upward. Magnetic mirror force transported ionospheric materials to feed the plasma sheet with atmospheric ions by increasing parallel temperatures if field-aligned potential accelerated the ionospheric source plasmas. But if the parallel potential is a barrier to the up flowing ionospheric source plasmas, plasma temperature is unchanged.

Field-aligned potentials were generated in the magnetosphere in such a way that the ionospheric potentials were amplified during their equatorial projection. This means that the

https://doi.org/10.5194/angeo-2020-92
Preprint. Discussion started: 4 January 2021

ionosphere responded to the initial dipolarization by returning the southward electric fields back to the dipolarization region in the magnetosphere. The southward electric fields in the ionosphere that became earthward electric fields in the plasma sheet further displaced the dipolarizing flux tube eastward which relaxed the radial inhomogeneity and intensified the dipolarization. This positive feedback loop may happen in magnetosphere and ionosphere system with the dipolarization region expanding in eastward to the down sector (Figure 5), like longitudinal expansion of field line dipolarization [e.g., Saka and Hayashi, 2017]. Earthward electric fields projected back to the dipolarization region in the plasma sheet would suppress westward expansion velocity in dusk sector. There may be asymmetric development of field line dipolarization in dawn-dusk directions.

6. Data availability. No data sets were use in this article.

7. Competing interest. The author declares that there is no conflict of interest.

References

Alfven, H. and Falthammar, C.-G.: Cosmical Electrodynamics, 2nd ed., Oxford University Press, New York, 1963.

Chiu, Y.T. and Schulz, M.: Self-consistent particle and parallel electrostatic field distributions in the magnetospheric-ionospheric auroral region, J. Geophys. Res. 83, 629-642, 1978.

Forget, B., Cerisier, J.-C., Berthelier, A., and Berthelier, J.-J.: Ionospheric closure of small-scale Birkeland currents, J. Geophys. Res., 96, 1843-1847, 1991.

Haerendel, G.: Plasma drifts in the auroral ionosphere derived from Barium release, in Earth magnetospheric processes, B.M. McComac (ed), D.Reidel Publishing Company, 246-257, 1972.

Kelley, M.C., Starr, J.A., and Mozer, F.S.: Relationship between magnetospheric electric fields and the motion of auroral forms, J.Geophys.Res., 76, 5256-5277, 1971.

Lui, A.T.Y.: Current disruption in the Earth's magnetosphere: Observations and models, J. Geophys. Res., 101, 13067-13088, 1996

McPherron, R.L., Russell, C.T., and Aubry, M.P.: Satellite studies of magnetospheric substorms on August 15, 1968: 9. Phenomenological model for substorms, J. Geophys. Res., 78, 3131-3148, 1973.

Nielsen, E., and Greenwald, R.A.: Variations in ionospheric currents and electric fields in association with absorption spikes during substorm expansion phase, J.Geophys.Res., 83, 5645-5654, 1978.

Persson, H.: Electric field along a magnetic line of force in a low-density plasma: Phys. Fluids, 6, 1756-1759, 1963.

Runov, A., Angelopoulos, V., Zhou, X.-Z., Zhang, X.-J., Li, S., Plaschke, F., and Bonnell, J.: A THEMIS multicase study of dipolarization fronts in the magnetotail plasma sheet, 116, A05216, doi:10.1029/2010JA016316, 2011.

Saka, O., Hayashi, K, and Thomsen, M.: First 10 min intervals of Pi2 onset at geosynchronous altitudes during the expansion of energetic ion regions in the nighttime sector, J. Atmos. Solar Terr. Phys., 72, 1100-1109, 2010.

Saka, O., and Hayashi, K.: Longitudinal expansion of field line dipolarization, J. Atmos. Solar Terr. Phys., 164, 235-242, 2017.

Saka, O.: A new scenario applying traffic flow analogy to poleward expansion of auroras, Ann. Geophys., 37, 381-387, 2019.

Saka, O.: The increase in the curvature radius of geomagnetic field lines preceding a classical dipolarization, Ann. Geophys., 38, 467-479, 2020.

Figure captions

Figure 1.
A schematic illustration of the plasma injection arising out of dynamic ionosphere (ionospheric injection). See text for detailed explanation.

Figure 2.
Equatorial projection of the ionospheric potentials (ϕ_i^+ and ϕ_i^-) from southern and northern hemispheres is illustrated. Ionospheric potentials are positive in higher latitudes (ϕ_i^+) and negative in lower latitudes (ϕ_i^-). Field-aligned potential amplified potential difference in the ionosphere during the equatorial projection ($\phi_m^{++} > \phi_i^+$, $\phi_m^{--} < \phi_i^-$). Earthward electric fields

https://doi.org/10.5194/angeo-2020-92
Preprint. Discussion started: 4 January 2021

are produced in the plasma sheet.

Figure 3.

Regions of velocity space ($\mathbf{\Sigma}$) occupied by the ionospheric species are shown. They were accelerated by the parallel potentials and magnetic mirror force: (A) electrons (ions) at 1,000 km altitudes for parallel potentials of 10 V (-10 V), (B) electrons (ions) at 10,000 km for 50 V (-50 V), (C) electrons (ions) at 20,000 km for 200 V (-200 V), and (D) electrons (ions) at geosynchronous altitudes for 500 V (-500 V). In the velocity space, ($v_{//}$, $v_{\perp}$) are normalized by the thermal velocity of respective particles (1 eV for this case).

Figure 4.

Same as Figure 3 but parallel potential behaved as potential barriers: (A) electrons (ions) at 1,000 km for parallel potentials of -10 V (10 V), (B) electrons (ions) at 10,000 km for -50 V (50 V), (C) electrons (ions) at 20,000 km for -200 V (200 V), and (D) electrons (ions) at geosynchronous altitudes for -500 V (500 V).

Figure 5.

Surface displacement at the inner boundary of the flux tube produced by the eastward flow *U* is shown as a solid line. This flow is triggered in the plasma sheet by the earthward electric fields (E_2) launched from equatorward projection of southward electric fields in the ionosphere (E_1). Eastward flow *U* further relaxed radial inhomogeneity to develop new dipolarization east of the original one. If this process is repeated, the dipolarization region may expand eastward consecutively.

https://doi.org/10.5194/angeo-2020-92
Preprint. Discussion started: 4 January 2021

Annales Geophysicae Discussions

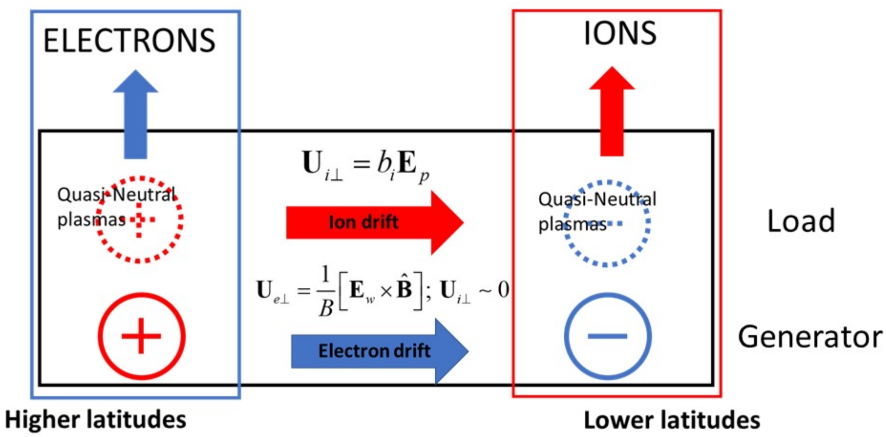

Figure 1

https://doi.org/10.5194/angeo-2020-92
Preprint. Discussion started: 4 January 2021

Annales Geophysicae
Discussions

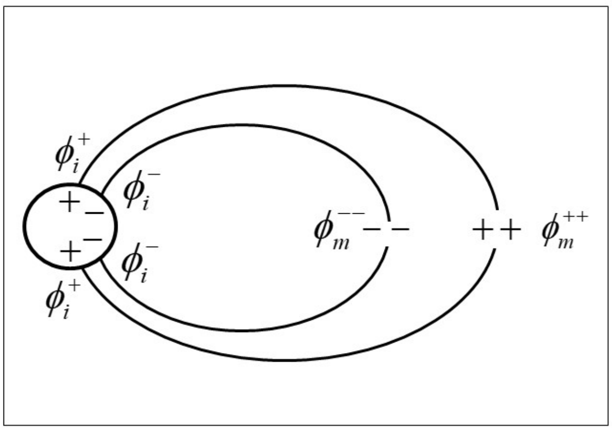

Figure 2

https://doi.org/10.5194/angeo-2020-92
Preprint. Discussion started: 4 January 2021

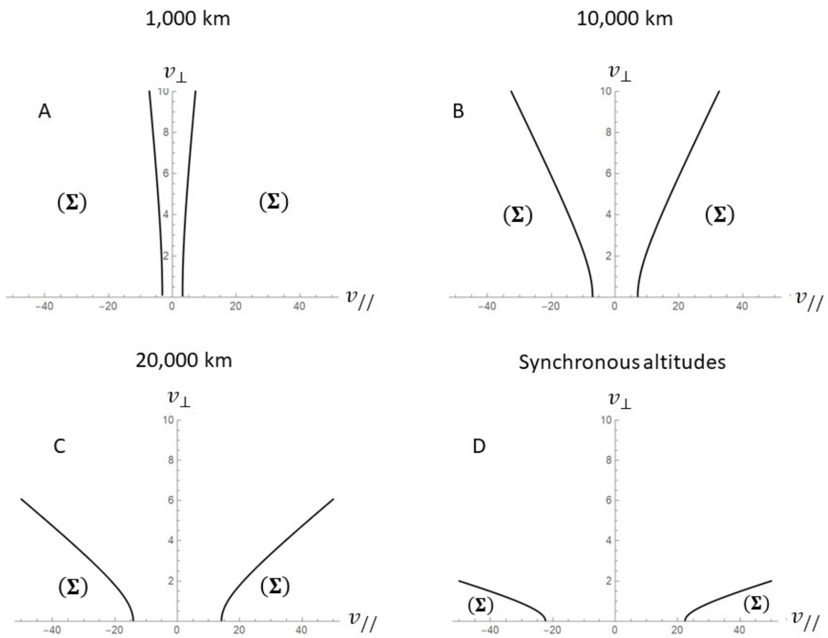

Figure 3

https://doi.org/10.5194/angeo-2020-92
Preprint. Discussion started: 4 January 2021

Annales Geophysicae Discussions Open Access

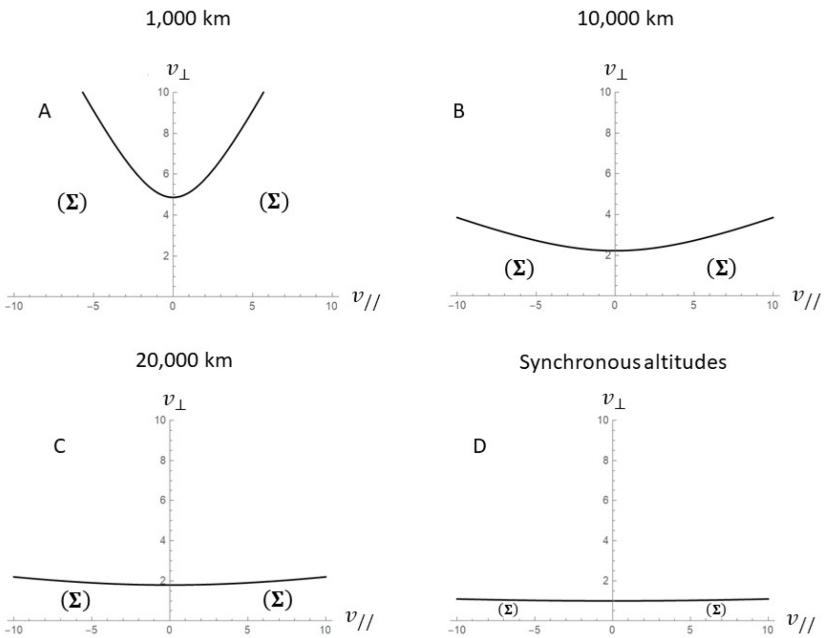

Figure 4

https://doi.org/10.5194/angeo-2020-92
Preprint. Discussion started: 4 January 2021

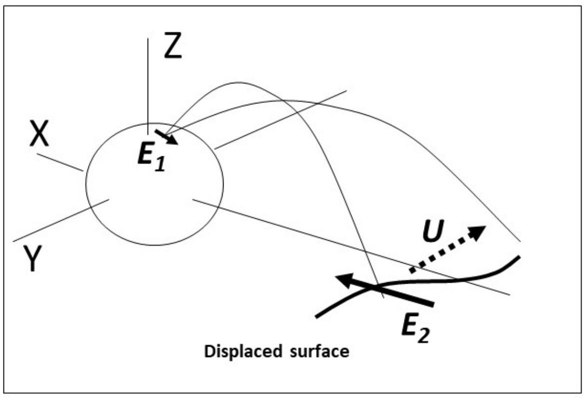

Figure 5